Electronic Supplementary Information (ESI)

Novel H_2 colourimetric indicator for screening the activity of H_2-generating bacteria and measuring their total viable count (TVC)

Lauren McDonnell, Christopher O'Rourke, Michaella Watson and Andrew Mills*

School of Chemistry and Chemical Engineering, Queens University Belfast, Stranmillis Road, Belfast, BT9 5AG, UK

S1 Examples of H_2 colourimetric indicators

Table S1. Examples of colourimetric H_2 indicators

Indicator[a]	**Colour change**[b]	**Ro or iR**[c]	**Notes**	**Ref**
Measurement of *dissolved* H_2				
MB+Pt colloid	B to C	Ro	All liquid indicator system; particles dispersed in solution.	1
Dyes + (Au-Pd) Nano-particles (NPs)	Rz(B to P); Rf (P to C); MR (Y to C); BTB (B to Y);	iR, except Rf	All liquid indicator system; particles dispersed in solution.	2
Rz with Pt/C particles	Rz(B to P)	iR	All liquid indicator system; particles dispersed in solution. Focus on the fluorescence of Rf produced by reduction of Rz by H_2, rather than colour change. Used to identify H_2 level in ambient gas.	3
Measurement of *gaseous* H_2				
Metals and metal oxides				
Pd on PDMS	Gry to W	Ro	Pd forms surface hydride upon exposure to H_2.	4
MoO_3 /Pd	Gry to B	iR	MoO_3/Pd vacuum deposited onto PTFE film) reduced to Mo(V) by H_2 produced by Mg implants	5
WO_3 /Pd	Gry to B	Ro	WO_3/Pd electrospray deposited onto Kapton tape; reduced to W(V) by H_2	6
PdO/TiO_2	Gry to Blk	iR	PdO reduced to Pd by H_2. Particles incorporated into silicone coated on polypropylene tape.	7
Pt/Mo-V_2O_5	Y to B	iR	Colour change due to reduction of V(V) to V(IV) by H_2 gas. Solgel of oxide deposited on indium tin oxide coated glass and sputtered with Pt.	8

Table S1. Examples of colourimetric H_2 indicators (cont'd)

Indicator[a]	Colour change[b]	Ro or iR[c]	Notes	Ref
Dyes				
Rz +(Au-Pd) NPs in gel	B to P	iR	Indicator and catalyst dispersed in agarose/alginate hydrogel., for monitoring Mg implants.	9
Powder, supraparticles (SPs) of SiO_2, Rz/Rf and H_2O.	B to P to C	iR, except Rf	Gas exposed to powder particles. Water is essential as dried out particles don't change colour.	10
Powder, supraparticles (SPs) of SiO_2, dyes and H_2O.	Rz(B to P); Rf (P to C); MR (Y to C); MB (B to C); TTZ (C to P)	Ro, except MR and TTZ	Gas exposed to powder particles. Water is essential as dried out particles don't change colour. Particles finally incorporated in a lacquer to show H_2 pipe leaks. No film stability results.	11
NTP/Ir complex catalyst	Y to Pp	iR	NTP/Ir complex dried on plasma -exposed polydimethylsiloxane (PDMS) sheet and then covered with another such sheet to create a tape. The tape works for ca. 14 days, after which it has lost water and stops working.	12
Dye/ Wilkinson's (Rh) catalyst	MB (G to Y)	iR	All liquid indicator system; particles dispersed in solution. The catalyst mediates the hydrogenation of the dye. Although many dyes are tested the fastest is MB.	13
WST dyes/Wilkinson's catalyst	C to Pp	iR	Liquid indicator/catalyst film separated from H_2-generating bacteria	14

a: Methylene blue (MB); Rz (resazurin); Rf (resorufin); MR (methyl red); BTB (bromothymol blue);DCIP (dichloroindophenol); TTZ (2,3,5-triphenyltetrazolium chloride); NTP (nitrotetrazolium blue chloride); WST (water soluble tetrazolium).

b: B (blue); C (colourless); Y (yellow); P (pink); Gry (grey); G (green); Blk (black);Pp (purple); W (white);

c: Ro (colour change reversed when exposed to oxygen/air; iR (colour change not reversed when exposed to oxygen or air).

References

1. T. Seo, R. Kurokawa and B. Sato, A convenient method for determining the concentration of hydrogen in water: use of methylene blue with colloidal platinum, *Med. Gas. Res.*, 2012, **2**, 1.

2. M. E. Smith, A. L. Stastny, J. A. Lynch, Z. Yu, P. Zhang and W. R. Heineman, Indicator dyes and catalytic nanoparticles for irreversible visual hydrogen sensing, *Anal. Chem.*, 2020, **92**, 10651-10658.
3. Y. Zhou, W. Wei, H. Su and W. Wang, Sensitively fluorescent detection of H_2 with resazurin hydrogenation reactions catalyzed by Pd/C nanocomposites, *Inorg. Chem. Commun.*, 2019, **106**, 139-143.
4. X. She, Y. Shen, J. Wang and C. Jin, Pd films on soft substrates: a visual, high-contrast and low-cost optical hydrogen sensor, *Light Sci. Appl.*, 2019, **8**, 4.
5. D. Zhao, T. Wang, W. Hoagland, D. Benson, Z. Dong, S. Chen, D. T. Chou, D. Hong, J. Wu, P. N. Kumta and W. R. Heineman, Visual H_2 sensor for monitoring biodegradation of magnesium implants in vivo, *Acta Biomater.*, 2016, **45**, 399-409.
6. J. Lee, H. Koo, S. Y. Kim, S. J. Kim and W. Lee, Electrostatic spray deposition of chemochromic WO_3-Pd sensor for hydrogen leakage detection at room temperature, *Sens. Actuators, B*, 2021, **327**, 128930.
7. K. Hwang, A. T-Raissi and N. Qin, Effect of pigment concentration and particle size of TiO_2 support on performance of chemochromic hydrogen tape sensor, *Int. J. Hydrogen Energy*, 2018, **43**, 9877-9883.
8. Y. R. Lu, H. H. Hsu, J. L. Chen, H. W. Chang, C. L. Chen, W. C. Chou and C. L. Dong, Atomic and electronic aspects of the coloration mechanism of gasochromic Pt/Mo-modified V_2O_5 smart films: an in situ X-ray spectroscopic study, *Phys. Chem. Chem. Phys.*, 2016, **18**, 5203-5210.
9. M. E. Smith, D. P. Rose, X. Cui, A. L. Stastny, P. Zhang and W. R. Heineman, A visual hydrogen sensor prototype for monitoring magnesium implant biodegradation, *Anal. Chem.*, 2021, **93**, 10487-10494.
10. J. Reichstein, S. Schötz, M. Macht, S. Maisel, N. Stockinger, C. C. Collados, K. Schubert, D. Blaumeiser, S. Wintzheimer, A. Görling, M. Thommes, D. Zahn, J. Libuda, T. Bauer and K. Mandel, Supraparticles for bare-eye H_2 indication and monitoring: design, working principle, and molecular mobility, *Adv. Funct. Mater.*, 2022, **32**.
11. J. Reichstein, P. Groppe, N. Stockinger, C. Cuadrado Collados, M. Thommes, S. Wintzheimer and K. Mandel, Safety through visibility: tracing hydrogen in colors with highly customizable and flexibly applicable supraparticle additives, *Adv. Mater. Technol.*, 2024, **9**, 2400441.

12. D. Fisher, M. Potter, P. Mandapati, M. W. Drover, S. Rondeau-Gagné and B. Mutus, Tetrazolium blue-based colorimetric sensor for hydrogen gas, *ACS Sustainable Chem. Eng.*, 2025, **13**, 15302-15310.
13. T. Katsuda, H. Ooshima, M. Azuma and J. Kato, New detection method for hydrogen gas for screening hydrogen-producing microorganisms using water-soluble wilkinson's catalyst derivative, *J. Biosci. Bioeng.*, 2006, **102**, 220-226.
14. P. S. Schrader, E. H. Burrows and R. L. Ely, High-throughput screening assay for biological hydrogen production, *Anal. Chem.*, 2008, **80**, 4014-4019.

S2 The bacteria

Escherichia coli (*E. coli*) is a Gram-negative, rod-shaped, facultative anaerobe, *i.e.* it can respire aerobically in the presence of O_2, but can switch to anaerobic respiration at low ambient levels of O_2.[1,2] Most *E. coli* strains are harmless and are found in gut flora where they produce vitamin K2 and inhibit pathogenic bacteria developing within the intestine.[1] However, some virulent strains of *E. coli* are responsible for causing a broad spectrum of illnesses and infections such as food poisoning, urinary tract infections, septicaemia, and neonatal meningitis.[1]

Under aerobic conditions in the growth medium used in this work, *E. coli* generates energy *via*,[3]

$$\text{Glucose } (C_6H_{12}O_6) + 6O_2 \rightarrow 6CO_2 + 6H_2O \qquad \text{(S1)}$$

In the absence of O_2, *E. coli* undergoes mixed acid and butanediol fermentation to metabolise glucose to formate, acetate, lactate, succinate, ethanol, 2,3-butanediol, CO_2 and H_2.[3] Literature reports that for every 100 mol glucose fermented by *E. coli*, 75 mol H_2 are produced.[3]

Klebsiella aerogenes (*K. aerogenes*) is a Gram-negative, rod-shape, facultative anaerobe.[4] It is found in the human gastrointestinal tract, and is common opportunistic pathogen in hospitals, causing respiratory, circulatory, and urinary infections in immunocompromised hosts.[4]

Like *E. coli*, under aerobic conditions, it utilises glucose and O_2 to produce CO_2 and water *via* reaction (S1). In the absence of O_2 it also undergoes mixed acid and butanediol fermentation to metabolise glucose to formate, acetate, lactate, succinate, ethanol, 2,3-butanediol, CO_2 and H_2.[3] For every 100 mol glucose fermented by *K. aerogenes*, 35.4 mol H_2 are produced.[3]

Enterobacter cloacae (*E. cloacae*) is a rod shaped, Gram-negative, facultative anaerobe. It is an emerging pathogen which is found in clinical settings and can cause a variety of infections in immunocompromised patients, such as urinary and respiratory infections.[5] Under aerobic conditions, it utilises glucose and O_2 to produce CO_2 and water *via* reaction (S1). In the absence of O_2 it also undergoes mixed acid and butanediol fermentation to metabolise glucose to formate, acetate, lactate, succinate, ethanol, 2,3-butanediol, CO_2 and H_2.[3]

Clostridium bifermentans (*C. bifermentans*) is an obligate anaerobic, spore-forming, Gram-positive bacterium. *C. bifermentans* is found in moderate temperature conditions including

in soil, marine environments, polluted waters, and human bodies.[6] While clinical cases are uncommon, it has been reported as an emerging pathogen that poses risk to health of humans as it can cause problems such as brain abscessus, inflammation of the uterus, infections of the joints and lymph nodes, and heart and lung conditions. Like other *Clostridium* species, it is a known H_2-producing bacteria and has been used to produce relatively larges amounts H_2 from wastewater sludge via fermentation in the literature.[7]

As it is an obligate anaerobe, *C. bifermentans* does not use O_2 to metabolise. It has been documented in the literature as producing a wide range of metabolites *via* fermentation, for example acetic, butyric and formic acids, ethanol, butanol, acetone, and gaseous products such as CO_2, H_2, and N_2.[8]

Pseudomonas putida (*P. putida*) is a Gram-negative, rod-shaped, saprophytic soil obligate aerobic bacterium[9] and is not a H_2 producer. In the nutrient broth used in this work, *P. putida* assimilates glucose through a cycle formed by enzymes of the Entner-Doudoroff, Embden-Meyerhof-Parnas and Pentose Phosphate pathways.[3,10]

References

1. *Escherichia coli*, https://globalrph.com/bacteria/escherichia-coli/https://globalrph.com/bacteria/escherichia-coli/, (accessed January 2026).

2. L. D. Clements, B. S. Miller, and U. N. Streips, Comparative growth analysis of the facultative anaerobes *Bacillus subtilis*, *Bacillus licheniformis*, and *Escherichia coli*, *Syst. Appl. Microbiol.* 2002, **25**, 284-286.

3. G. Gottschalk, Bacterial Metabolism, Springer-Verlag, New York, USA, 2nd edn, 1986.

4. H. Gu, Q. Cai, X. Dai, H. Wang, W. Xu, X. Cao and Y. Ye, A case report of *Klebsiella aerogenes*-caused lumbar spine infection identified by metagenome next-generation sequencing, *BMC Infect. Dis.*, 2022, **22**, 616.

5. *Enterobacter cloacae*, Enterobacter Cloacae: Facts, Symptoms, Treatment | STD.GOV Blog (std-gov.org), (accessed January 2026).

6. T. S. Sasi Jyothsna, L. Tushar, Ch. Sasikala and Ch. V. Ramana, *Paraclostridium benzoelyticum* gen. nov., sp. nov., isolated from marine sediment and reclassification of *Clostridium bifermentans* as *Paraclostridium bifermentans* comb. nov. Proposal of a new genus *Paeniclostridium* gen. nov. to accommodate *Clostridium sordellii* and *Clostridium ghonii*, *Int. J. Syst. Evol. Microbiol.*, 2016, **66**, 1268-1274

7. C. C. Wang, C. W. Chang, C. P. Chu, D. J. Lee, B. V. Chang, and C. S. Liao, Producing hydrogen from wastewater sludge by *Clostridium bifermentans*, *J. Biotechnol.,* 2003, **102**, 83-92.

8. K. Leja, K. Myszka and K. Czaczyk, The ability of *Clostridium bifermentans* strains to lactic acid biosynthesis in various environmental conditions, *SpringerPlus*, 2013, **2**, 44.

9. Pseudomonas putida, https://en.wikipedia.org/wiki/Pseudomonas_putida, (accessed January 2026).

10. L. Molina, R. La Rosa, J. Nogales, F. Rojo, *Pseudomonas putida* KT2440 metabolism undergoes sequential modifications during exponential growth in a complete medium as compounds are gradually consumed, *Environ. Microbiol*., 2019, **21**, 2375-2390.

S3 Growth media

Table S2. Compositions of the different media used in this work

Bacterium	**Classification**	**Growth medium**	**Composition (in 1 L water)**
E. coli *K. aerogenes* *P. putida*	Facultative anaerobe Obligate aerobe	Nutrient broth (NB)	Prepared using a standard formulation.[1] • 10 g glucose • 5 g casein yeast peptone • 5 g sodium chloride
		Nutrient agar	10 g agar were added to the above nutrient broth.
E. cloacae	Facultative anaerobe	Modified nutrient broth	Combination of a standard nutrient broth,[1] with a modified version of a broth used for enhancing H_2 production of the bacterium in the literature.[2] • 10 g glucose • 5 g casein yeast peptone • 5 g sodium choride • 0.2 g magnesium sulphate • 2 g sodium bicarbonate
		Modified nutrient agar	10 g agar were added to the above nutrient broth.
C. bifermentans	Obligate anaerobe	Thioglycollate broth (TGB)	29 g thioglycollate broth powder (USP alternative).[3] 29 g thioglycollate broth powder contains: • 15 g pancreatic digest of casein • 5 g yeast extract • 5.5 g dextrose • 2.5 g sodium chloride • 0.5 g L-Cystine • 0.5 g sodium thioglycollate
		Tryptic soy agar (TSA)	30 g tryptic soy broth powder[4] and 10 g agar. 30 g tryptic soy broth powder contains: • 17 g casein peptone (pancreatic) • 3 g soya peptone (papain digest.) • 5 g sodium chloride • 2.5 g D(+)-glucose monohydrate • 2.5 g dipotassium phosphate

Various liquid growth media were used throughout this work, and the preparation of each followed a general method which involved dissolving the various reagents listed in Table S2, in a 1 L borosilicate glass reagent bottle containing 1 L water. Once fully dissolved, each growth medium was sterilized by autoclave at 121°C for 15 mins and then stored in a fridge before use. Each growth medium was prepared fresh every few days.

To make the solid agar growth plate counting media for *E. coli*, *K. aerogenes*, *E. cloacae*, or *P. putida*, 10 g agar were added to 1 L of the liquid growth medium and, once dissolved, the solution was autoclaved at 121 °C for 15 min, and then allowed to cool to 52 °C in air. The hot liquid agar was then poured into large 90 x 15 mm Petri dishes,[5] and the plates allowed to cool to room temperature. The final plates were refrigerated and used as required.

In contrast to the above, the solid agar growth plate counting medium used with the obligate anaerobe *C. bifermentans* was a tryptic soy agar recommended by the retailer of the bacterium.[6] This medium was prepared by adding 30 g tryptic soy broth powder and 10 g agar to a 1 L borosilicate glass reagent bottle containing 1 L water. Once all the components had dissolved, the solution was autoclaved at 121 °C for 15 min, allowed to cool to 52 °C in air and then, poured into the 90 x 15 mm Petri dishes and allowed to cool to room temperature. The final plates were refrigerated and used as required.

References

1. L. McDonnell, D. Yusufu, and A. Mills, CO_2-Based micro-respirometry for measuring bacterial load under aerobic and anaerobic conditions, *Analyst*, 2024, **149**, 5582-5590.

2. Q. Zhang, S. You, Y. Li, X. Qu and H. Jiang, Enhanced biohydrogen production from cotton stalk hydrolysate of *Enterobacter cloacae* WL1318 by overexpression of the formate hydrogen lyase activator gene, *Biotechnol. Biofuels*, 2020, **13**, 20200522.

3. Thioglycollate broth (USP Alternative), https://www.sigmaaldrich.com/GB/en/product/sial/70157?msockid=15bb1e28b5636274187c0c90b43b6388, (accessed January 2026).

4. Tryptic soy broth, Tryptic Soy Broth - Dehydrated Culture Media GranuCult® prime, EP, JP, USP, granular, irradiated, suitable for aseptic process simulation | Sigma-Aldrich, (accessed January 2026).

5. ISO 4833–2, ISO 4833–2:2013, Microbiology of the food chain- horizontal method for the enumeration of microorganisms- part 2: colony count at 30 °C by the surface plating technique, International Organization for Standardization, Geneva, 2013.
6. *Clostridium bifermentans* retailer, https://www.microbiologics.com/0828K, (accessed January 2026).

S4 Preparation of bacteria stock dispersions and determination of their concentration using the plate count method (PCM)

E. coli*, *K. aerogenes*, *E. cloacae, and P. putida

To produce a primary stock culture of the different bacteria listed above, a KWIK-STIK containing a pure population of either *E. coli*, *K. aerogenes*, *E. cloacae*, or *P. putida* was gently swabbed across the surface of the solid agar in a 90 x 15 mm Petri dish.[1] The inoculated culture plate was immediately incubated at 30 °C overnight, after which there was visible growth of single colonies of bacteria; subsequently, the plate was wrapped in Parafilm® and refrigerated until needed.

The process of making an overnight stock of a liquid culture of *E. coli, E. cloacae*, *K. aerogenes, or P. putida* was as follows: a single colony of the bacterium was taken from the primary culture plate using a sterile inoculating loop and suspended in 10 mL of NB in a 15 mL Falcon® tube, which was then incubated overnight at 30 °C. The bacterial liad, i.e., total viable count (TVC) of the resulting overnight culture, *ca.* 10^8 CFU/mL, was confirmed using the aerobic plate count method (PCM), as described below.[2]

Serial 1-in-10 dilutions of the overnight bacterial culture in NB were used to produce suspensions of initial inoculum concentrations of *ca.* 10^8-10^1 CFU/mL of the bacteria; these dilutions were prepared fresh on the day of use. These serial diluted dispersions of the bacteria under test were then used as the 1 mL inocula in the H_2 indicator-based microrespirometry work for measuring TVC.

An aerobic version of the PCM was carried out for *E. coli*, *E. cloacae*, *K. aerogenes*, and *P. putida* bacteria. This involved inoculating 3 agar plates with 0.1 mL of the assumed '*ca.* 10^3 CFU/mL' dilution, and another 3 agar plates inoculated with 0.01 mL of the same dilution, which were spread across the plate with an L-spreader; the plates were incubated at 30 °C overnight. After this period, there was visible growth of single colonies of bacteria on each plate, which could then be counted, an average of the plate counts taken, and the results used to estimate the microbial load/TVC of the original overnight culture stock.[1]

C. bifermentans

To produce a primary stock culture, a KWIK-STIK containing a pure population of the obligate anaerobic bacteria *C. bifermentans* bacteria was gently swabbed across the surface of the

solid tryptic soy agar in a 90 x 15 mm Petri dish.[1] The inoculated culture plate was immediately incubated at 37 °C for 48 hours under an anaerobic atmosphere; this was achieved by incubating the plates inside an anaerobic jar (Thermo Scientific™ Oxoid™ AnaeroJar™ 2.5L, Thermo Fisher Scientific, Massachusetts, USA), which was sealed with an anaerobic gas-generating sachet inside (Thermo Scientific™ Oxoid™ AnaeroGen™ 2.5L Sachet, Thermo Fisher Scientific, Massachusetts, USA). After this period there was visible growth of single colonies of *C. bifermentans* bacteria; subsequently, the plate was wrapped in Parafilm® and refrigerated inside an anaerobic jar, containing an anaerobic gas-generating sachet, until required.

The process of making a liquid stock culture of *C. bifermentans* was as follows: firstly, thioglycollate broth (USP alternative, Merck, Gillingham, UK), which contains the reducing agent sodium thioglycolate[3] which removes any O_2 in the broth, was prepared fresh on the day of use. 13 mL of this broth were poured while still hot, *ca.* 70 °C, into a 15 mL Falcon® tube, and the broth allowed to cool to room temperature inside the Falcon tube to minimise the O_2 saturation of the broth.[3] Then, a single colony of *C. bifermentans* was taken from the primary culture plate, using a sterile inoculating loop, and suspended in the cooled thioglycollate broth; the Falcon® tube was then incubated for 48 hours at 37 °C, in an anaerobic jar containing an anaerobic gas-generating sachet. The loading of the resulting liquid stock solution, typically *ca.* 10^7 CFU/mL, was confirmed using a modified anaerobic version of the aerobic PCM,[4] in which inoculated agar plates for use in the anaerobic PCM were incubated for 48 hours at 37 °C, under anaerobic conditions in an anaerobic jar, after which there was visible growth of single colonies of *C. bifermentans* bacteria, which were counted and the microbial load/TVC of the original liquid stock solution then calculated.

References

1. Microbiologics KWIK-STIK™, https://www.microbiologics.com/item-type/Product/product-format/KWIK-STIK-2-Pack,KWIK-STIK-6-Pack, (accessed January 2026.

2. ISO 4833–2, ISO 4833–2:2013, Microbiology of the food chain- horizontal method for the enumeration of microorganisms- part 2: colony count at 30 °C by the surface plating technique, International Organization for Standardization, Geneva, 2013.

3. DSMZ Cultivation of Anaerobes document, Folie 1, (accessed January 2026).

4. M. Yamagata, Anaerobic plate count (spread and pour plate method), in *Laboratory Manual on Analytical Methods and Procedures for Fish and Fish Products*, ed. H. Hasegawa and K. Miwa, Singapore: Marine Fisheries Research Department, Southeast Asian Fisheries Development Center, 2nd edn, 1992, pp E9.1-9.5.

S5 The H_2 indicator: additional details

A TEM micrograph of the Pt colloid used to make the H_2 indicator is illustrated in Fig. S1.

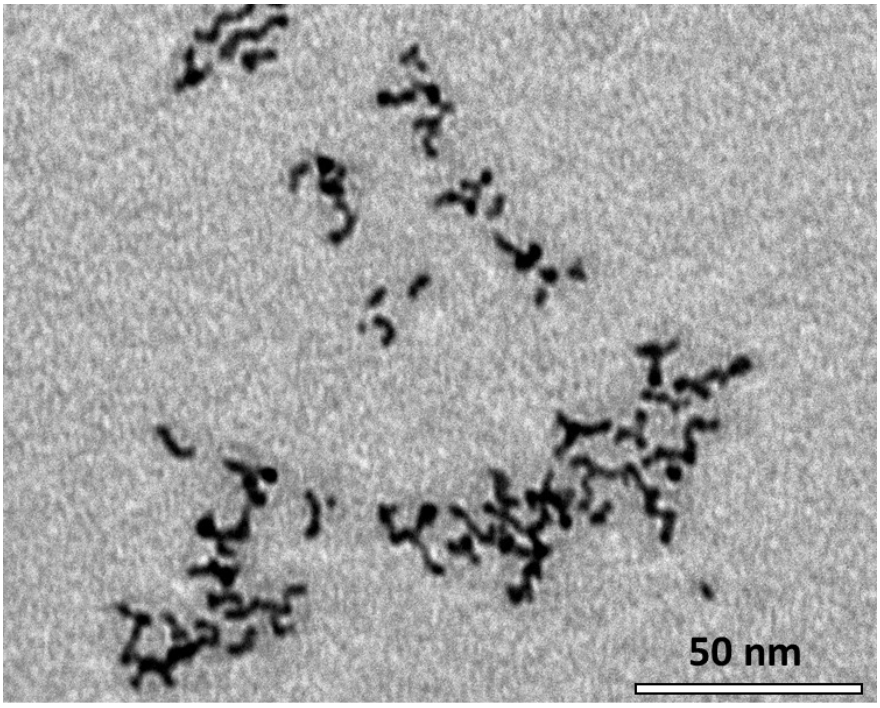

Fig. S1 TEM of the Pt colloid used to make the H_2 indicator.

Fig. S2 illustrates a histogram plot of number of particles versus Pt particle size, , derived from the TEM images of the Pt colloid, such as illustrated in Fig. S1, from which an average Pt particle size of 2.2 ± 0.5 nm was calculated.

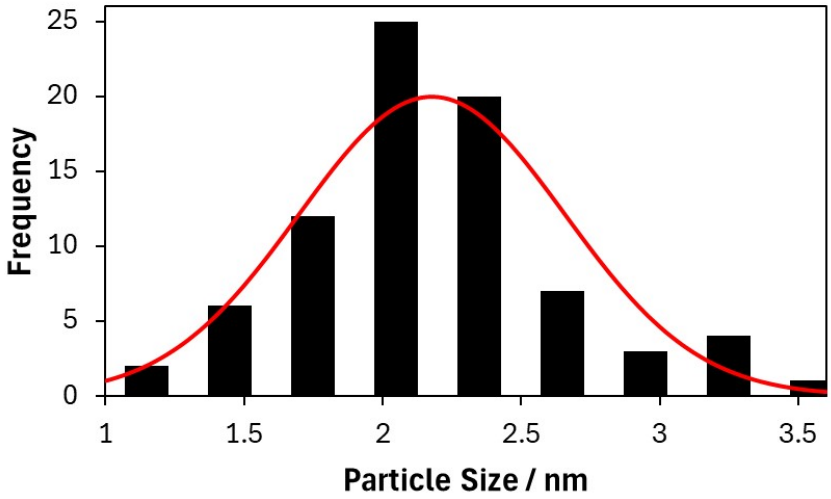

Fig. S2 Histogram plot of the number of particles (frequency) versus Pt particle size based on TEM images of the Pt colloid.

The inert supporting substrate used in the work was Tyvek™ which is a fibrous, highly gas-permeable, inert, high-density polypropylene material,[1] with a white colour that provided a strong contrast to the blue-coloured H_2 indicator and so aided the high-definition photography of the indicator.

A photograph of the final (laminated) H_2 indicator, before (blue) and after (colourless) exposure to H_2 is illustrated in Fig. S3. Once rendered colourless by exposure to H_2, the original colour of the indicator returned only after exposure to air and not, for example, upon exposure to a non-oxidising gas, such as Ar.

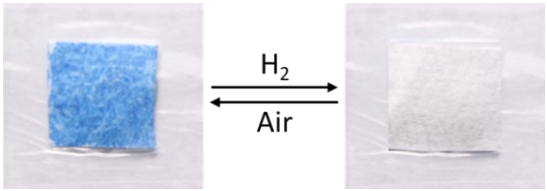

Fig. S3 Photographs of the H_2 indicator before (blue) and after (colourless) exposure to 100% H_2.

The overall blue to colourless colour change observed for the H_2 indicator upon exposure to H_2, as illustrated above in Fig. S3 , can be summarised by the following reaction equation,

$$\underset{\text{Blue}}{MB} + H_2 \xrightarrow{Pt} \underset{\text{colourless}}{LMB} \qquad \text{(S2)}$$

In the absence of O_2, LMB is a very stable species but, in its presence, it is readily oxidised back to MB,

$$LMB + + 0.5O_2 \longrightarrow MB + H_2O \qquad \text{(S3)}$$

The structures of MB and LMB are given in Fig. S4.

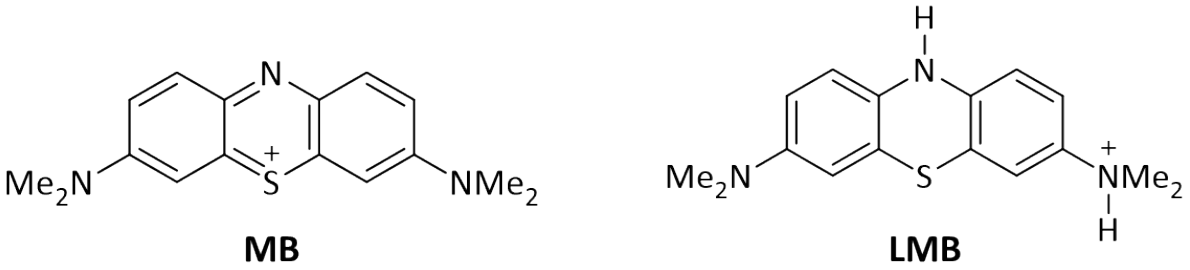

Fig. S4. Structures of methylene blue(MB) and *leuco*-methylene blue (LMB)

Evidence for the above reaction was obtained by coating the H_2 indicator onto a quartz disc and recording its UV/Vis spectrum before and after exposure, the results of which are illustrated in Fig. S5. Before exposure the blue-coloured H_2 indicator film, exhibited an absorption spectrum typical of the monomer and dimer forms of MB, with absorption peaks at, 292, 607 and 665 nm.[2,3] When bleached by exposure to H_2, the UV/Vis spectrum of the colourless H_2 indicator film was that of LMB, with a major peak at 262 nm.[2,4]

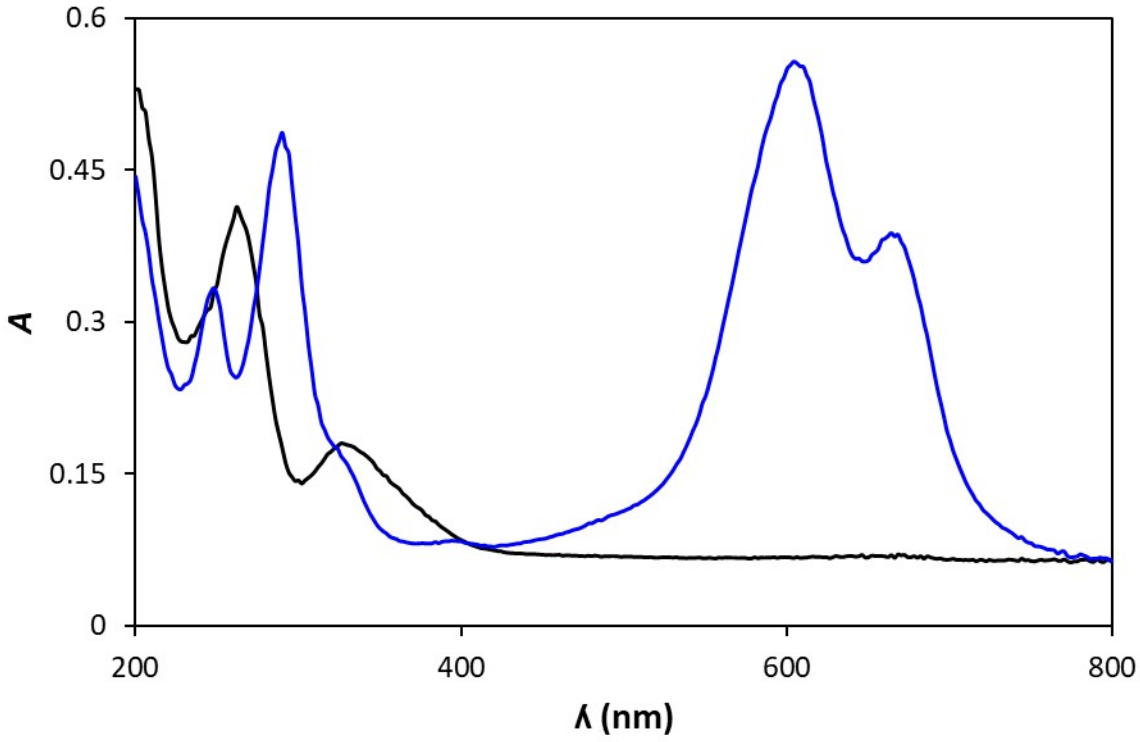

Fig. S5 UV/Vis absorption spectra of the H_2 indicator film on quartz before (blue line) and after (black line) exposure to H_2.

References

1. What is Tyvek ®?, what is Tyvek® | DuPont™ Tyvek® for Design, (accessed January 2026).
2. N. R. de Tacconi, J. Carmona and K. Rajeshwar, Reversibility of photoelectrochromism at the TiO_2/methylene blue interface, *J. Electrochem. Soc.*, 1997, **144**, 2486-2490.
3. E. Braswell, Evidence for trimerization in aqueous solutions of methylene blue, *J. Phys. Chem.*, 1968, **72**, 2477-2483.
4. A. Mills and J. Wang, Photobleaching of methylene blue sensitised by TiO_2: an ambiguous system?, *J. Photochem. Photobiol., A*, 1999, **127**, 123-134.

S6 Digital colour analysis (DCA) and an *A'* vs *A* study using H_2 sensor

In digital colour analysis, DCA, the values of the red, green, and blue (RGB) components of the image are first determined using a simple programme (ImageJ)[1,2] and, in the case of the H_2 indicator used here, the value for the indicator's apparent absorbance, *A'*, is calculated *via* the following expression,

$$A' = \log\{255/\mathrm{RGB(red)}\} \quad \text{(S4)}$$

where RGB(red) is the measured value of the red parameter in the RGB-analysed image of the sensor.[1] Previous work with numerous colour-based indicators has demonstrated that in each case the indicator's value of *A*', as measured using photography/DCA, is directly proportional to its actual absorbance, *A*, as measured using UV-Vis spectrophotometry, at the wavelength of maximum absorbance. To demonstrate this feature, the H_2 indicator ink was coated onto a clear film of polyethylene terephthalate (PET), using K-bar #3. PET was used in this one case, as it is clear and therefore allows the value of *A'* and *A* to be measured at the same time. Although, LDPE was used in the H_2 indicator, its role is as a gas permeable membrane, GPM, and not as a support substrate, because it is very hydrophobic and, consequently, has a very low surface energy (29.3 mJ m^{-2}),[3] which causes the H_2 ink to reticulate, and prevents the production of an even coating. In contrast, PET is much less hydrophobic, as evidenced by its high surface energy, 72.4 mJ m^{-2},[4] which allows the H_2 indicator ink to be coated onto its surface.

To speed up the process of colour recovery the final dried H_2-indicator ink on PET was NOT laminated and we refer to this indicator as a naked (non-laminated) H_2 indicator. Thus, the blue-coloured naked H_2 indicator was placed in the inside wall of a 1 cm cuvette and the headspace flushed with 100% H_2 gas, whereupon the sensor turned colourless. The cuvette was then very loosely stoppered so that over the period of 1 h all the H_2 leaked out, so that the headspace in the cuvette returned to that of just air and the H_2 indicator returned to its original (no H_2 present) blue colouration. In this experiment, as the $\%H_2$ level in the headspace decreased, the digital photographic image of the naked H_2 indicator film, and its corresponding UV-Vis spectrum, were recorded simultaneously as a function of time. Fig. S6(a) illustrates some of the recorded digital images of the H_2 indicator as a function of time, from which, using DCA and eqn (S4), the *A*' value associated with each photographic image was determined. Fig. S6(b) illustrates the simultaneously measured UV-Vis absorbance

spectra of H_2 indicator, from which absorbance, *A*, values, due to D^-, measured at 665 nm were taken. Fig. S6(c) shows the subsequent linear plot of *A*' vs *A* which demonstrates that, in this work using a H_2 indicator, *A*' is proportional to *A,* and so proportional to the concentration of the oxidised form of the dye, i.e., proportional to [MB].

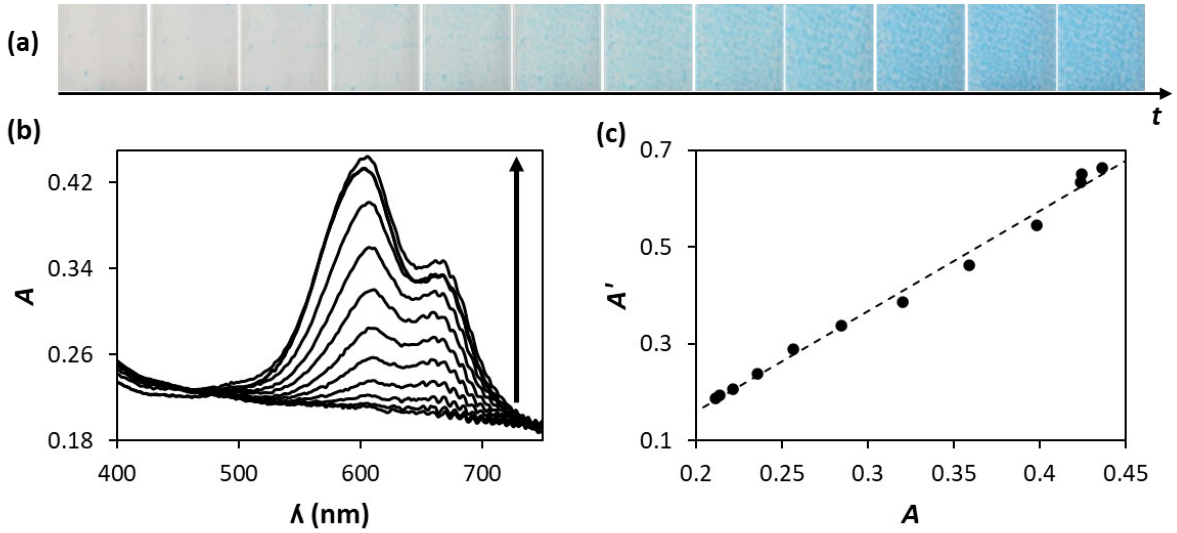

Fig. S6 (a) Digital photographs of a laminated H_2 indicator (*the* H_2 indicator), initially saturated with 100% H_2, and so bleached, then allowed to lose its H_2 to ambient air over time, recorded, from left to right, every 30 min. (b) Spectral changes recorded at the same time for naked H_2 indicator, during the same H_2 – air exchange process experiment. The spectra were recorded (from bottom to top) every 30 min after the initial bleaching by H_2. (c) Plot of apparent (DCA) absorbance, *A'*, vs real (spectrophotometric) absorbance, *A,* (at 665 nm) for the H_2 indicator film.

For completeness, the same experiment as described above was conducted using a 'naked' H_2 indicator, the results for which are illustrated below in Fig. S7. As in Fig S6, the results for the 'naked' H_2 indicator in Fig. S7 reveal a linear plot of *A*' vs *A* which demonstrates that, in this work using a laminated H_2 indicator, *A*' is proportional to *A,* and so proportional to the concentration of the oxidised form of the dye, i.e., proportional to [MB].

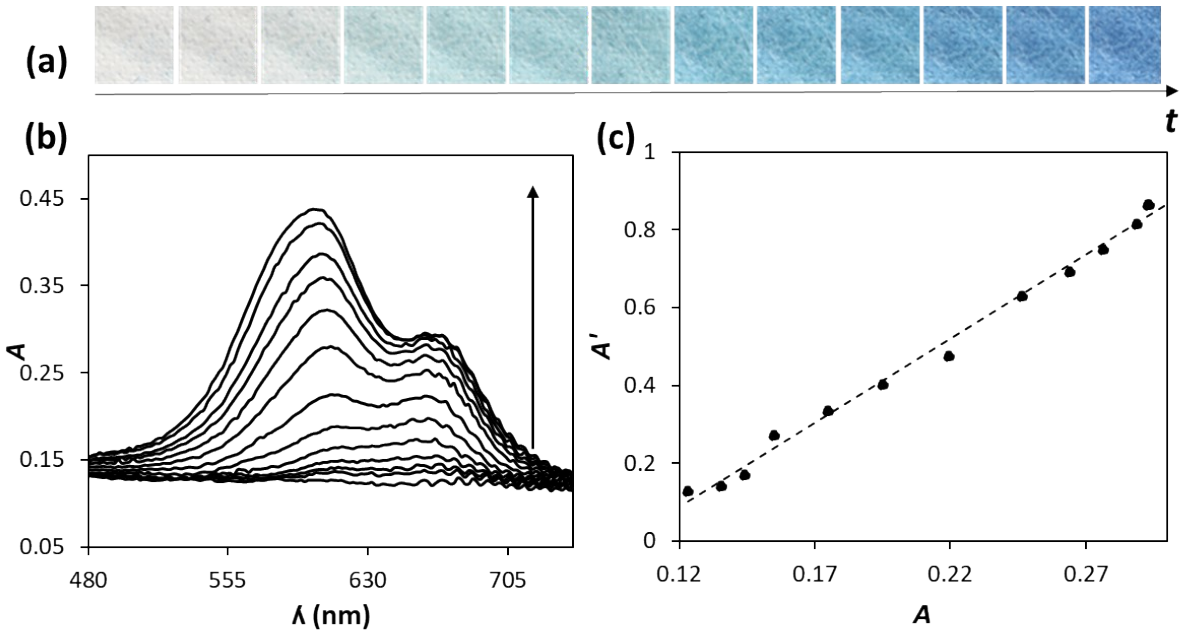

Fig. S7 (a) Digital photographs of a 'naked' H_2 indicator (not laminated), initially saturated with 100% H_2, and so bleached, then allowed to lose its H_2 to ambient air over time, recorded, from left to right, every 30 min. (b) Spectral changes recorded at the same time for naked H_2 indicator, during the same H_2 – air exchange process experiment. The spectra were recorded (from bottom to top) every 30 min after the initial bleaching by H_2. (c) Plot of apparent (DCA) absorbance, *A'*, vs real (spectrophotometric) absorbance, *A,* (at 665 nm) for the H_2 indicator film.

In addition, the same indicator response and recovery experiment as described in Fig. 1 for the laminated H_2 indicator, was also carried out using a naked (no LDPE lamination layers) H_2 indicator, with the results illustrated in Fig. S8. The 50% response time to 23.9% H_2 and then 23.9% O_2 were 0.3 and 6.8 mins. Figs. S8(c) and (d) also illustrate, respectively, the response and recovery *A'* vs time profiles for the laminated H_2 indicator, taken from Fig. 1(d), red points, for which values of 0.7 and 7.5 min were gleaned for the 50% response times to H_2 and then O_2.

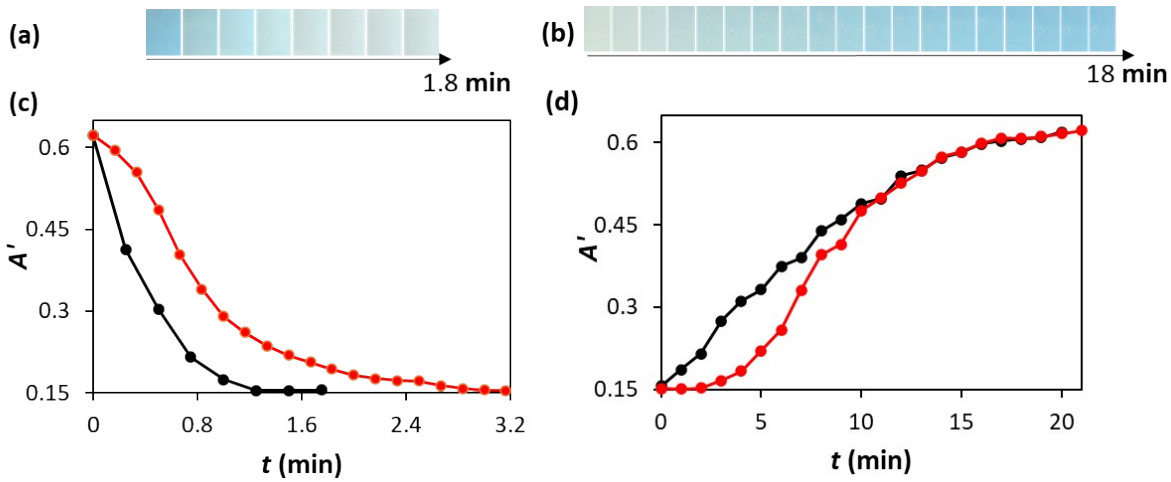

Fig. S8 (a) photographs of the naked H_2 indicator upon exposure to 23.9% H_2 as a function of time, *t.* (b) subsequent photographs of the naked indicator in an Ar atmosphere, upon exposure to 23.9% O_2, as a function of *t*, (c) and (d) *A'* vs time plots generated *via* DCA of the photographs in (a) and (b), respectively, black points. Also illustrated in (c) and (d) are the respective response and recovery *A'* vs time profiles for the laminated H_2 indicator, taken from the first and last sections of Fig. 1(d), red points.

References

1. D. Yusufu, A. Mills, Spectrophotometric and digital colour colourimetric (DCC) analysis of colour-based indicators, *Sens. Actuators, B*, 2018, **273**, 1187-1194.

2. Image J, https://imagej.nih.gov/ij/download.html, (accessed January 2026).

3. S. Habib, M. Lehocky, D. Vesela, P. Humpolicek, I. Krupa and A. Popelka, Preparation of progressive antibacterial LDPE surface via active biomolecule deposition approach, *Polymers (Basel)*, 2019, **11**, 1704.

4. D. Papakonstantinou, E. Amanatides, D. Mataras, V. Ioannidis and P. Nikolopoulos, Improved surface energy analysis for plasma treated PET films, *Plasma Processes Polym.*, 2007, **4**, S1057-S1062.

S7 Kinetic studies of the H_2 indicator, test of stability in growth medium

Following on from the initial kinetics study of the response (to H_2) and recovery (in O_2) kinetics of the H_2 indicator outlined in Section 3.1 of the main text, the same system was used to study these kinetics as a function of ambient $\%H_2$ and $\%O_2$. As before the 'reactor', containing the indicator was a 1 cm cuvette (volume 4.18 mL) fitted with a rubber septum, and in all cases, before the different volumes of 100% H_2, or 100% O_2, were injected, the cell was sparged with Ar. Note that, in the O_2 kinetics study, as a precursor to the injection of O_2, in order to get the MB in the H_2 indicator in its reduced (LMB) form, the cell was first sparged for 1 min with 100% H_2, before being sparged with Ar. The different volumes of 100% H_2, or O_2, injected into the cuvette containing only Ar and the indicator in its blue (oxidised/MB) form, or colourless (reduced/LMB) form, respectively, were: 0.25, 0.35, 0.50, 0.75 and 1.0 mL so that the ambient % gas levels produced were 6.0, 8.9, 12.0, 17.9 and 23.9%, respectively. The results of this work in the form of the *A'* vs *t* profiles for these different injection volumes of H_2 and O_2 are illustrated in Figs S9(a) and (b), respectively. Each decay (or growth) *A*' vs *t* profile yielded a value for t_{50}, the time taken for the indicator to lose (or regain) half its colour, t_{50}. These values were used to generate the $1/t_{50}$, vs %gas straight line plots illustrated in Fig. S9(c) for H_2 and O_2. The ratio of the gradients indicates that for the H_2 indicator the kinetics of reaction (2) are *ca.* 6x's bigger (faster) that of reaction (3).

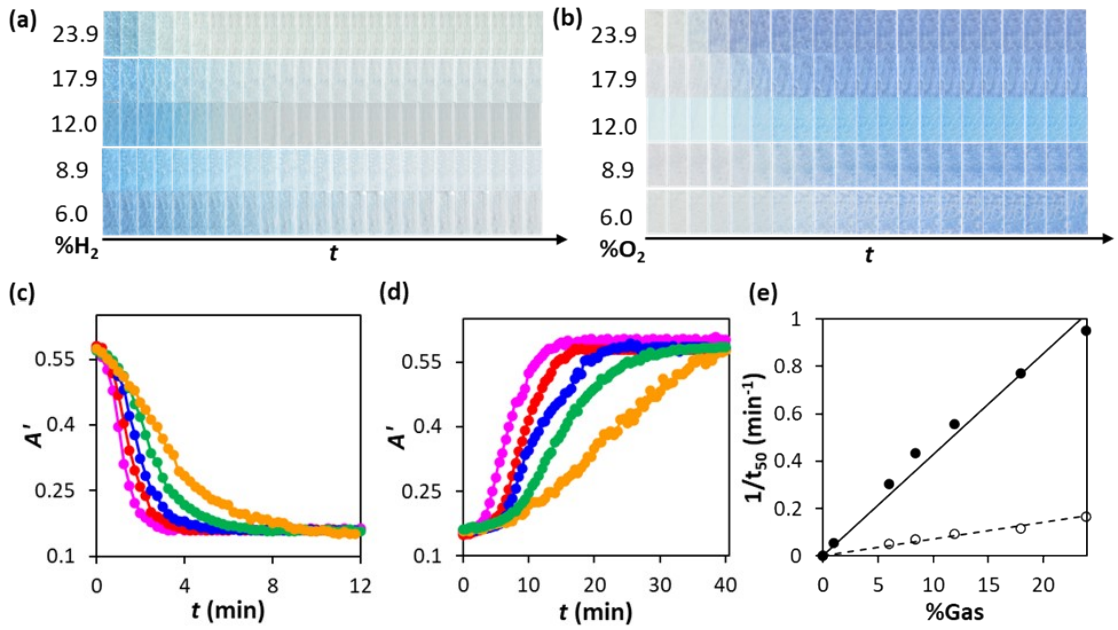

Fig. S9 Photographs of the H_2 indicator after injection of different volumes of 100% (a) H_2 and, after flushing the cell with Ar, (b) O_2 gas, in a sealed 1 cm cuvette (4.39 mL) containing the H_2 indicator The different injected gas volumes produced the following %gas levels, 6.0, 8.9, 12.0, 17.9 and 23.9 % in the cell. (c) The photographs in (a), coupled with DCA, were used generate the *A'* vs *t* profiles illustrated in (c); the yellow (slowest), green, blue, red and pink (pasted) coloured decay curves were due to the presence of 6.0, 8.9, 12.0, 17.9 and 23.9 $\%H_2$, respectively. Similarly, the photographs in (b), coupled with DCA, were used generate the *A'* vs *t* profiles illustrated in (d); the yellow (slowest), green, blue, red and pink (pasted) coloured decay curves were due to the presence of 6.0, 8.9, 12.0, 17.9 and 23.9 $\%O_2$, respectively. (d) Plot of $1/t_{50}$ vs % gas for injections of H_2 (solid points; gradient = 0.039 min^{-1} $\%H_2^{-1}$) and O_2 (open circles; gradient = 0.0065 min^{-1} $\%O_2^{-1}$).

In all this work, unless stated otherwise, the temperature of the H_2 indicator was maintained at 37.0 $\pm$ 0.2°C using a Heratherm™ incubator (Thermo Scientific, Massachusetts, USA). Careful control of the temperature is essential in microrespirometry since bacterial growth kinetics and the gas sensor sensitivity are temperature sensitive. To demonstrate the temperature sensitivity of the H_2 indicator, the same experiment as described in Fig. S9(a), was carried out at 18 °C, the results of which are illustrated in Fig. S10(a). Different values of t_{50} were derived from the measured *A*' vs *t* decay curves, illustrated in Fig. S10(a), for the different $\%H_2$ levels, and the subsequent plot of $1/t_{50}$ vs $\%H_2$ (at 18 °C) are illustrated in Fig. 10(b), red data points, along with the $1/t_{50}$ vs $\%H_2$ (at 37 °C) data set from Fig. S9(e), black data points; the gradients of the lines of best fit to the two data sets were 0.013 and 0.039

min^{-1} $\%H_2^{-1}$, respectively. An Arrhenius equation analysis of these two gradients indicates an activation energy of ca. 43 kJ mol^{-1}, for reaction (2).

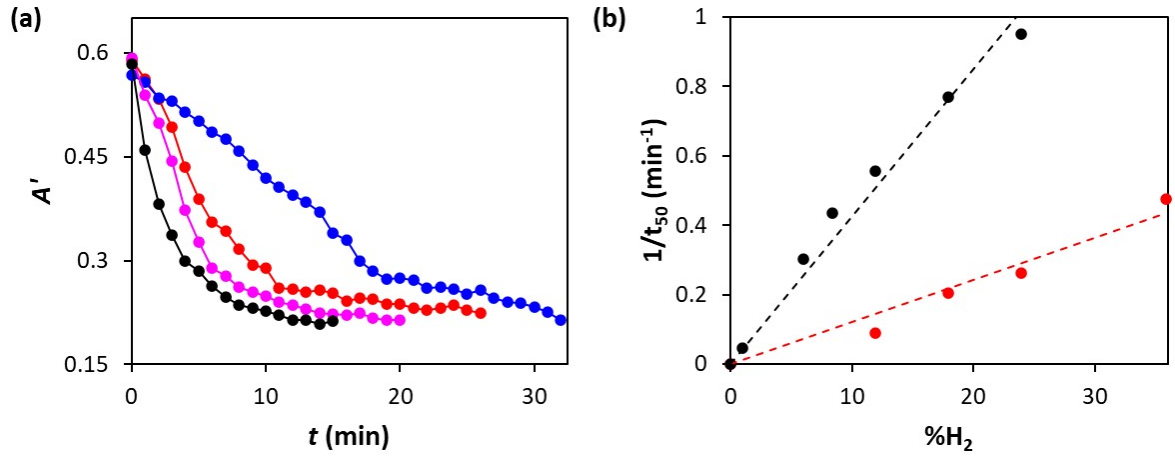

Fig. S10 (a) *A'* vs *t* profiles recorded at 18 °C, upon injection of different volumes of 100% H_2 gas, in a sealed 1 cm cuvette (4.39 mL) containing the H_2 indicator and, initially, an ambient atmosphere of Ar. The different injected gas volumes produced the following %gas levels, 12.0, 17.9, 23.9 and 35.9%, %, and generated the blue (slowest), red, pink and black (fastest) coloured decay curves when H_2 was injected. (c) Plot of $1/t_{50}$ vs % gas for injections of H_2 at 18 °C (red points; gradient = 0.013 min^{-1} $\%H_2^{-1}$) and at 37 °C (black points; gradient = 0.039 min^{-1} $\%H_2^{-1}$).

Although not the primary focus of this paper it is also possible to use the H_2 indicator to detect H_2, by injecting the latter into a stream of air and monitoring the change in colour it produces in the indicator placed downstream. A simple illustration of the setup is given in Fig. 11(a), which comprised a 14 mL glass 'reactor' through which air was flowed at 60 mL min^{-1}, and into which different volumes of H_2 could be injected, and downline from which was placed the naked H_2 indicator (as it is slightly faster responding than the laminated indicator) which was photographed as a function of time. The photographs recorded using the above system were used to produce a series of *A*' vs *t* peaks of height which increased with increased volume of injected H_2. A typical example of the recorded photographs and associated *A*' vs *t* peak for a 4 mL injection of H_2 are illustrated in Figs. S11(b) and (c), respectively. In this short study, the volumes of H_2 injected, V_{H2}, were varied from 4 to 1 mL and the resulting straight-line plot of peak height change in *A*', ΔA', versus V_{H2} is illustrated in Fig. S11(d). The results of this very limited study show how the H_2 indicator might be used to detect H_2 quantitatively, but clearly more work is required to establish fully its performance and possible limitations as a quantitative method for measuring gaseous H_2 levels in air.

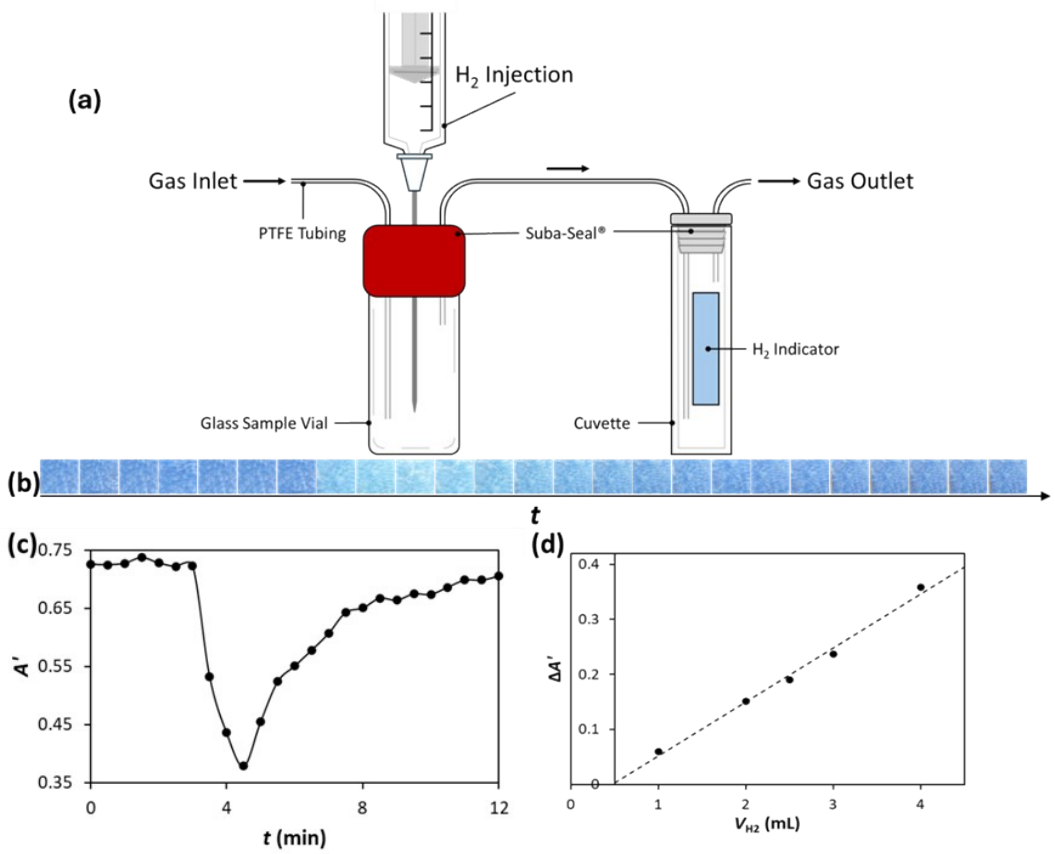

Fig. S11 (a) Schematic of the crude, gas flow system, using a naked H_2 indicator, used for measuring injected volumes of H_2, V_{H2}. (b) typical set of photographs associated with the injection of 4 mL H_2 into the system in (a), and (c) the variation in *A*' as a function of time after injection, *t*, calculated using the photographs in (b) and DCA. (d) Plot of the change in peak height, ΔA', vs. V_{H2}. The broken line is that of best fit to the data, with a gradient and intercept of 0.098 ± 0.005 mLH_2^{-1} and -0.046 ± 0.014, respectively; and correlation coefficient = 0.9798.

To demonstrate the efficacy of the H_2 indicator as a sensor for pure H_2, the same experiment as used to generate the data in Fig. S9, was carried out using different levels of H_2, with the H_2 indicator's being restored by exposure to air. The resulting plot of *A*' vs *t* is illustrated in Fig. S12(a), from which the subsequent straight-line plot of $1/t_{50}$ vs $\%H_2$, over the range 23.9 – 0.04 $\%H_2$ was constructed and is illustrated in Fig. S12(b). The correlation coefficient of the line of best fit to the data, *r*, was 0.9932, the gradient $\pm$ standard deviation, $m \pm \sigma$, were 0.040 $\pm$ 0.002 min^{-1} $\%H_2^{-1}$ and the limit of detection ($3.3x\sigma/m$) was 0.16 $\%H_2$.

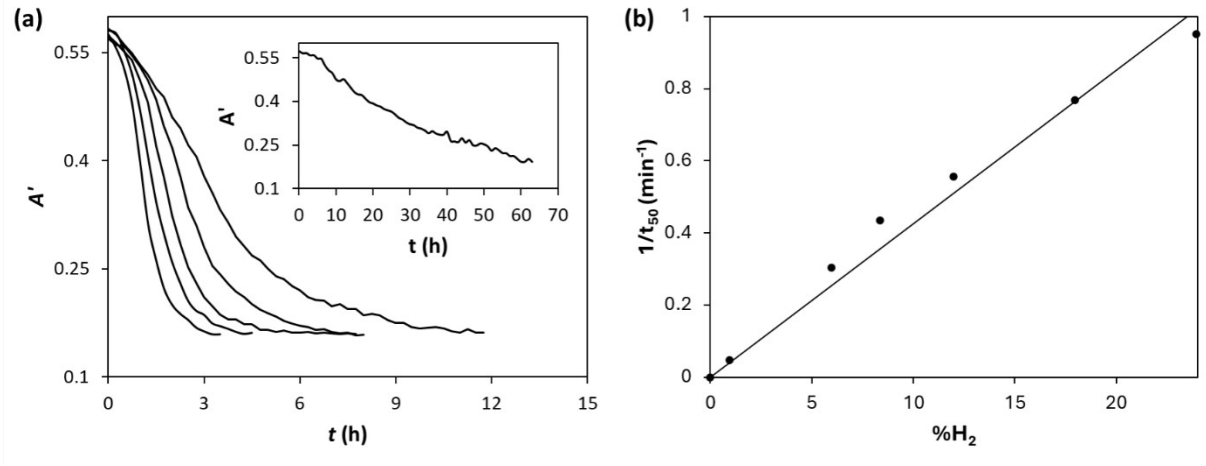

Fig. S12. (a) *A'* vs *t* profiles recorded upon injection of different volumes of 100% H_2 gas, as in Fig. S10, which produced the following different %H_2 gas levels, 6.0, 8.9, 12.0, 17.9 and 23.9 %, and generated, from left to right, the slowest to fastest decay curves, respectively; the insert plot in (a) is the recorded *A'* vs *t* decay curve for 0.04 %H_2. (b) Subsequent reciprocal plot of the t_{50} data derived from the decay curves in (a) vs % H_2 gas in cell.

In another set of experiments the long-term stability of the H_2 indicator in growth medium was tested. Thus, the H_2-indicator was placed inside a 15 mL Falcon tube to which 10 mL of nutrient broth (NB), containing 3.97 x 10^{-4} M sodium sulfite, were then added. This solution represents the typical growth medium used in both the screening and TVC studies reported here. The Falcon tube with indicator was then sealed and incubated at 37 °C for 72 h and the H_2 indicator photographed every 4 h. The indicator stayed the same blue colour over the monitored period and the DCA of recorded photographs of the indicator were used to produce the plot of *A'* vs incubation time, *t*, illustrated in Fig. S13, from which an average value of *A'* = 0.56 ± 0.01, was calculated.

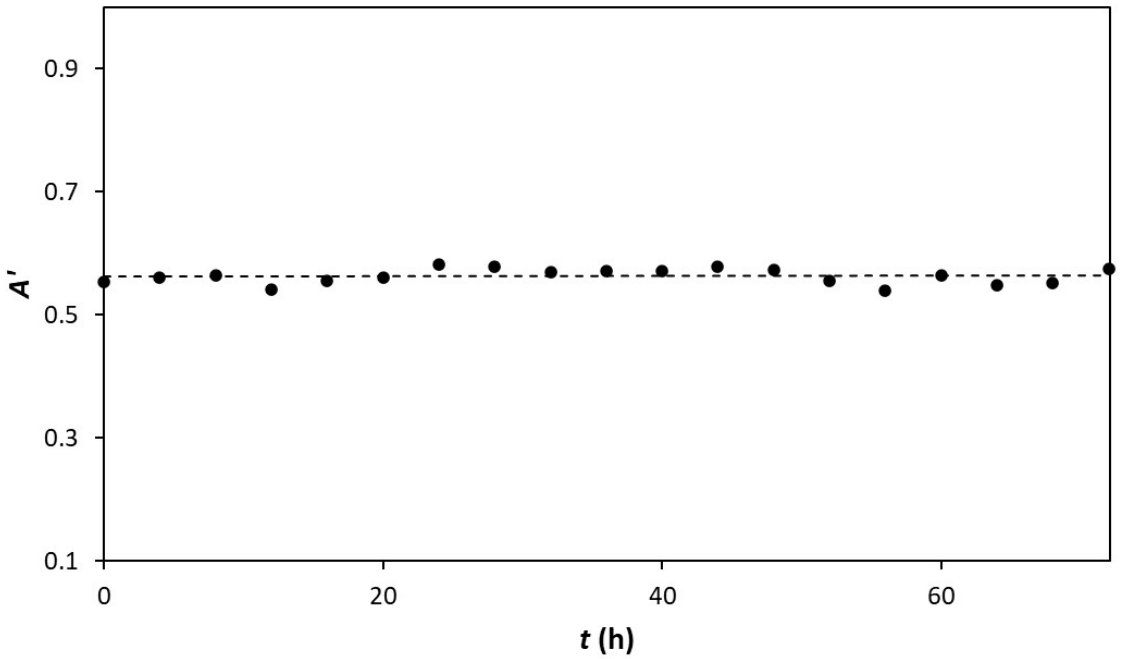

Fig. S13. Plot of the apparent absorbance, *A'*, of a H_2 indicator vs time when placed in 10 mL of nutrient broth containing 50 mg (3.97×10^{-4} M) of Na_2SO_3 and incubated at 37 °C for 72 h.

The above results show that the H_2 indicator is stable in the growth medium for at least 3 days at 37 °C.

S8 H_2 evolution and bacterial growth kinetics

The continuous logistic equation is a popular, basic model used to describe bacterial growth kinetics. It is based on the idea that the growth rate of a given population, introduced into a virgin environment, is proportional to the size of the population at any growth time, *t*, *N*(*t*), and the remaining material resources in the habitat.[1] Thus,

$$dN(t)/dt = kN(t)[1- (N(t)/N_{max})] \quad \text{(S5)}$$

where N_{max} is the maximum number of bacteria the habitat can support and *k* is a proportionality constant that reflects how well the bacteria grows in the habitat. An integrated form of eqn (S5) is,

$$N(\tau_u) = N_{max}/[1 + A^*\exp(-\tau_u)] \quad \text{(S6)}$$

where N_o is the initial population of the bacteria, and $A^* = (N_{max}/N_o - 1)$ and τ_u (= kt), is a unitless measure of time. In most of the work reported here, A* can be approximated to equal (N_{max}/N_o) since the latter ratio is usually >> 1.

If we define a time point (the threshold time, TT), τ_{uTT}, at which N_τ has reached a defined fraction (1/*x)* of N_{max}, where $x > 1$, then it can be shown that

$$\tau_{uTT} = \ln(A^*/(x-1)) \quad \text{(S7)}$$

Given, eqn (S6) and $A^* = N_{max}/N_o >> 1$, it also follows that,

$$\ln(N_o) = \ln(N_{max}/(x-1)) - \tau_{uTT} \quad \text{(S8)}$$

which, very importantly, predicts a plot of $\ln(N_o)$ vs τ_{uTT} will be a good straight line with a gradient = -1. Note: every value of N_o will be paired with value of τ_{uTT}, defined by eqn S8. In practice this means if a measured incubation time, TT (units: h), is measured for different values of N_o, at which $N_\tau = N_{max}/x$, then a plot of $\ln(N_o)$ vs TT will be a good straight line of gradient *k*.

If we assume, at any time τ_u, the rate of H_2 evolution, r_{H2}, is proportional to the concentration of bacteria, $N(\tau)$, then it follows that

$$r_{H2} = a/[1 + A^*.\exp(-\tau_u)] \quad \text{(S9)}$$

where $a = k_H N_{max}$, and k_H is the rate constant associated with H_2 production. The integrated form of eqn (S9) is

$$[H_2]_{\tau u} = a.\ln[\exp(\tau_u) + A^*] - a.\ln(A^*) \quad \text{(S10)}$$

which predicts that at $\tau_u = \tau_{uTT}$, the concentration of H_2 produced is fixed, and independent of N_o, since,

$$[H_2]_{\tau uTT} = a.\ln(x/(x\text{-}1)) \quad \text{(S11)}$$

This means, regardless of the initial inoculation concentration, N_o, the amount of H_2 produced at the time point, TT (unitless), at which $N_{\tau u} = N_{max}/x$, will always be the same value and the smaller the fraction (*i.e.*, the bigger the value x) the smaller the concentration of H_2, $[H_2]_{\tau uTT}$, as expected. It seems reasonable to assume that during any H_2 microrespirometry run, when the original blue colour of the H_2 indicator is reduced by 50%, this is because it has been exposed to a certain (*i.e.* fixed) concentration of H_2, $[H_2]_{50}$; the incubation time at which this colour change point occurs is t_{50} (units: h) Eqn (S11) shows that if the $[H_2]$ is fixed, then so is x and eqn (S8) applies. Thus, if the value of t_{50} is measured for a variety of initial inoculant concentrations, N_o, then a plot of $\log(N_o)$ vs t_{50}, should be a straight line with a negative gradient, with a slope which reflects the growth kinetics of the bacteria. Note it is NOT necessary to know the value of $[H_2]_{50}$, just as in O_2 μR-TVC it is not necessary to know the concentration of O_2 when the lifetime of the O_2 is midway between its initial and final values, it is simply necessary that a specific colour (say at 50% colour change point), or lifetime (say at 50% change in lifetime point), is always associated with a fixed concentration of H_2 , or O_2, respectively

References

1. M. G. Corradini and M. Peleg, Estimating non-isothermal bacterial growth in foods from isothermal experimental data, *J. Appl. Microbiol.*, 2005, **99**, 187-200.

S9 The H_2 microrespirometry method and H_2 indicator reproducibility and affect of potential interfering species.

To test the reproducibility of the H_2 indicator and the microrespirometry method, ten H_2 indicators, made on different days, were used to monitor the H_2 produced by a 1 mL inoculation of 10^4 CFU/mL *E. coli* in 9 mL of growth medium, as described above. The results of this work, a superimposed, series of near-identical *A*' vs *t* profiles, are illustrated below in Fig. S14(a), from which ten, very similar, values for t_{50} were determined, see Fig. S14(b), with an average value of 10.3 $\pm$ 0.3 h. The set of near identical, *A*' vs *t* profiles illustrated in Fig. S14(a) and the low % standard deviation, 3%, in t_{50}, indicates a high level of reproducibility, both in terms of the production of the H_2 indicator and the micro-respirometry methodology employed.

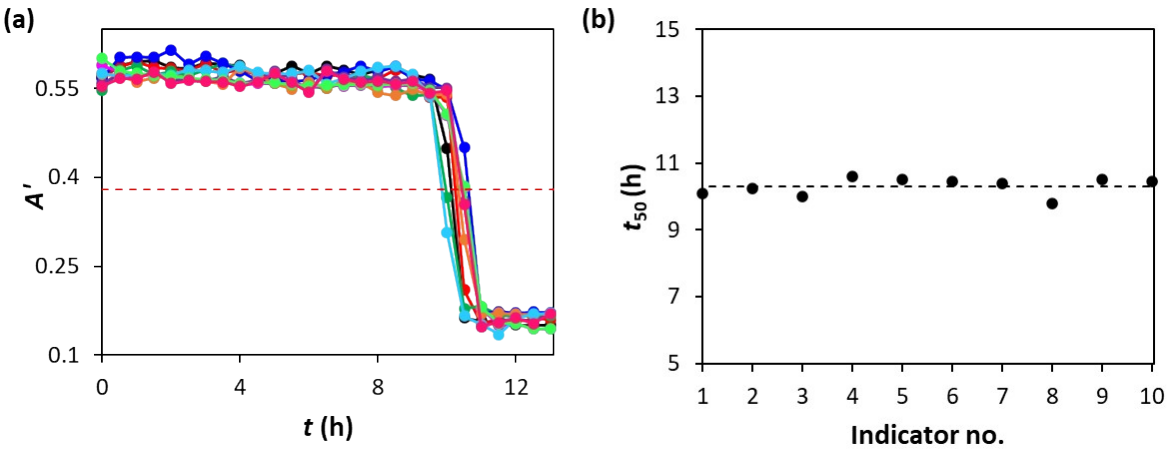

Fig.S14 Plot of *A*' vs *t* profiles produced using 10 different H_2 indicators, when used to monitor the H_2 evolution vs incubation time profile produced when 9 mL of growth medium were inoculated with 1 mL of 10^4 CFU/mL *E. coli*. The incubation temperature was 37°C.

As the H_2 indicator is protected by the gas-permeable LDPE layers, the indicator is unaffected by any non-volatile potential interfering species generated as the bacteria metabolise. However, possible interfering gaseous, and volatile, water-soluble species, such as H_2S, CO_2, CH_4, ethanol, acetic acid, formic acid and 1,2, butanediol, were tested, typically at a level of 1 %. In this work, the indicator was placed in water either saturated with 1% of the gaseous species under test, or containing 1% of the water-soluble species under test. In each case, the indicator was left in the solution for 30 min before being then removed, washed thoroughly and then tested for response in a typical microrespirometry experiment in which

9 mL of growth medium were inoculated with 1 mL of 10^4 CFU/mL *E. coli*, all incubated at 37 ^oC A H_2S level of 0.1% was used as this is the level is considered highly toxic for The photographs recorded as a function of incubation time arising from this work are illustrated in Fig. S15(a) from which the *A'* vs *t* profiles, associated with the different, potential interferants tested, that are illustrated in Fig. S15(b), were generated. These results show that when exposed to 1%, or less, of each of the potential interferants tested, all but H_2S do not change the response characteristics of the H_2 indicator, which is perhaps not surprising given the nature of key reactions, (1) and (2). The slowed response of the H_2 indicator after exposure to 1% H_2S for 30 min is not unexpected, given sulfides are generally recognised as Pt catalyst poisons. Thus, although the H_2 indicator would most likely to be able to detect H_2 generated by H_2-generating bacteria, it could not be used to assess the TVC if a significant (1%) level of H_2S was present. Thus, when using H_2 μR to assess the TVC of a H_2 producing bacterium, as in this work, the growth medium should not contain inorganic sulfur compounds (such as sulfate) nor sulfur-containing amino acids, such as cysteine. Since H_2S is a highly toxic gas, it is also not surprising that most reported H_2-producing bacterial systems, avoid its production by using a renewable biomass with a high content of carbohydrate, such as glucose, as noted in the Introduction.

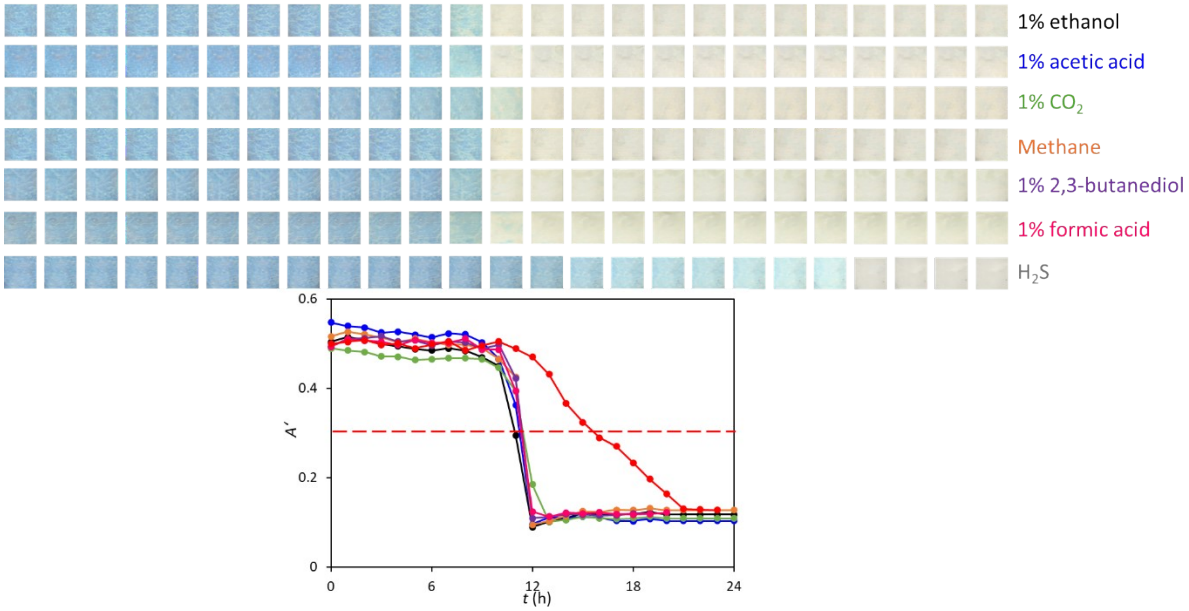

Fig. S15 Each indicator was first exposed for 30 min to 1% of the named, potential interferent and then tested for response using a typical microrespirometry system, comprising 9 mL of growth medium, inoculated with 1 mL of 10^4 CFU/mL *E. coli*. (a) Photographs of the H_2

indicator's response to the H_2 generated by the *E. coli* as a function of incubation time, *t*. (b) *A*' vs *t* profiles, associated with the different interferants tested, derived from the photographs in (a), using DCA.

In addition, in the above, 'before and after 3 days soaking' experiment the H_2 indicator's response to the H_2 generated in a typical H_2 microrespirometry experiment was measured and found to be unchanged. In this work, a 1 mL inoculum of 10^4 CFU/mL *E. coli* was added to 9 mL of growth medium, incubated at 37 ^oC and the indicator photographed as a function of incubation time; the two sets of photographs, for the H_2 indicator before and after 3 days soaking at 37 ^oC, are illustrated in Figs S16(a) and (b), respectively. These photographs were then analysed using DCA and yielded the two almost identical *A*' vs *t* plots, as illustrated in Fig. S16(c). The superimposable forms of these two *A*' vs *t* plots demonstrates that the response characteristics of the H_2 indicator are unchanged after soaking it in growth medium at 37 ^oC for 3 days.

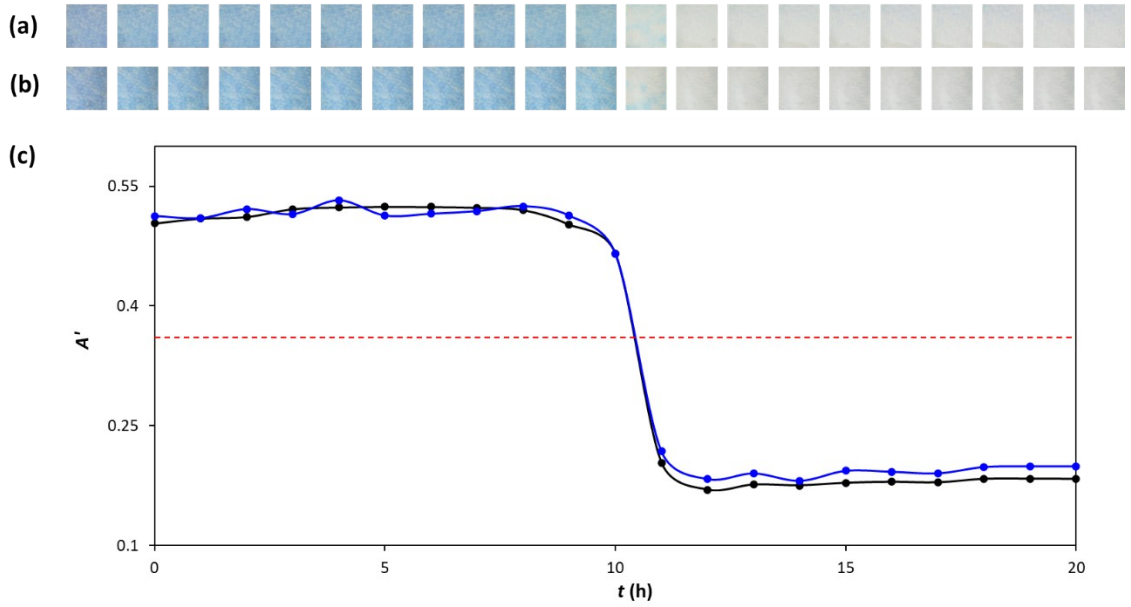

Fig. S16 Photographs of the H_2 indicator as a function of incubation time, *t*, when placed in a 10 mL of growth medium, containing 10^4 CFU/mL *E. coli*, (a) before and (b) after previously soaking the indicator for 3 day at 37 ^oC. (c) *A*' vs *t* plots, black and blue lines, generated *via* DCA analysis of the photographs in (a) and (b), respectively.

The same, simple microrespirometry test system, in which 1 mL inoculum of 10^4 CFU/mL *E. coli* was added to 9 mL of growth medium, incubated at 37 ^oC and the indicator photographed as a function of incubation time, was also used to test the stability of the H_2 indicator when

stored in a cool, dark place. Although this is an on-going test, initial results show that the indicator's response characteristics remain unchanged for at least 1 month, see Fig. S17.

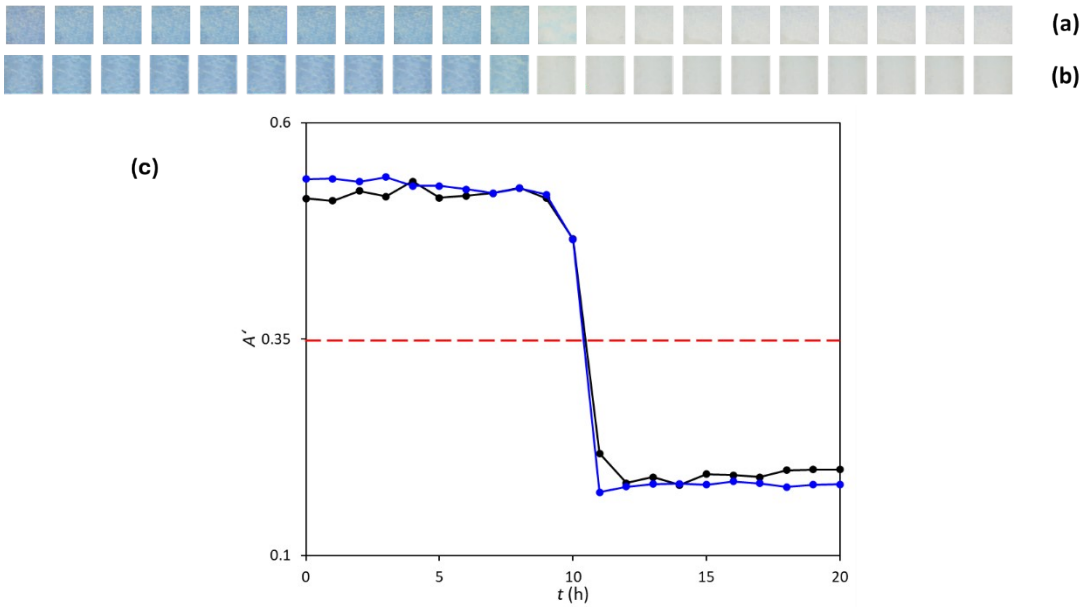

Fig. S17 Photographs of the H_2 indicator as a function of incubation time, *t*, when placed in a 10 mL of growth medium, containing 10^4 CFU/mL *E. coli*, (a) before and (b) after 1 month storage in a cool, dark place. (c) *A*' vs *t* plots, black and blue lines, generated *via* DCA analysis of the photographs in (a) and (b), respectively.

S10 H_2 microrespirometry for measuring TVC for bacteria other than *E. coli*

K. aerogenes

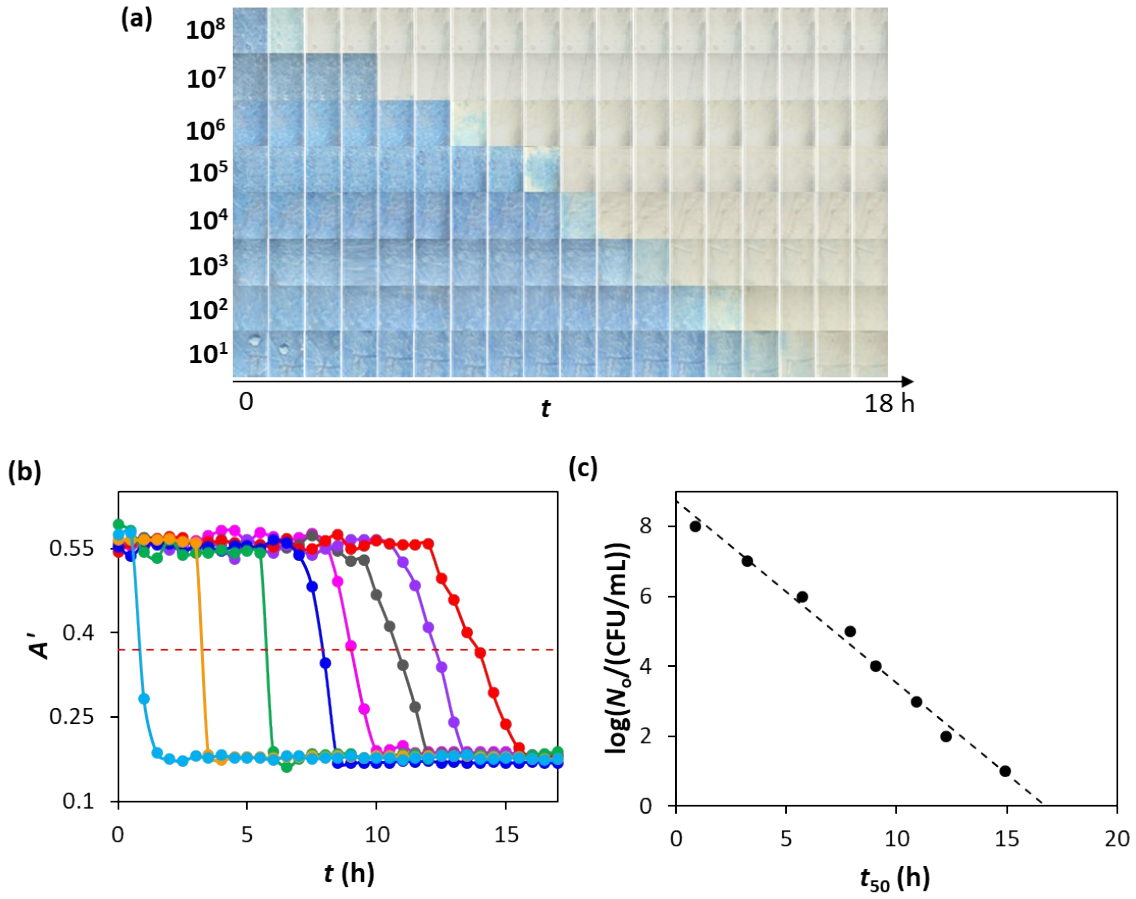

Fig. S18. (a) Photographic images of the H_2 indicator as a function of incubation time, t, in a typical set of H_2 μR-TVC runs, in which the 9 mL of growth medium were inoculated with a 1 mL *K. aerogenes* sample with a bacterial load spanning the range (from left to right) 10^8 – 10^1 CFU/mL. (b) A' vs t reverse 'S' shaped profiles calculated from the photos illustrated in (a) using DCA and eqn (4), for initial inocula of (from left to right): 10^8, 10^7, 10^6, 10^5, 10^4, 10^3, 10^2 and 10^1 CFU/mL, respectively. The broken horizontal red line highlights the half-way colour change value, which is used to identify the value of t_{50} associated with each reverse 'S' shape profile/log(N_o/(CFU/mL)) value. (c) Subsequent straight line, calibration graph plot of log(N_o/(CFU/mL)) vs t_{50}, derived from (b). Incubation temperature: 37 °C.

E. cloacae

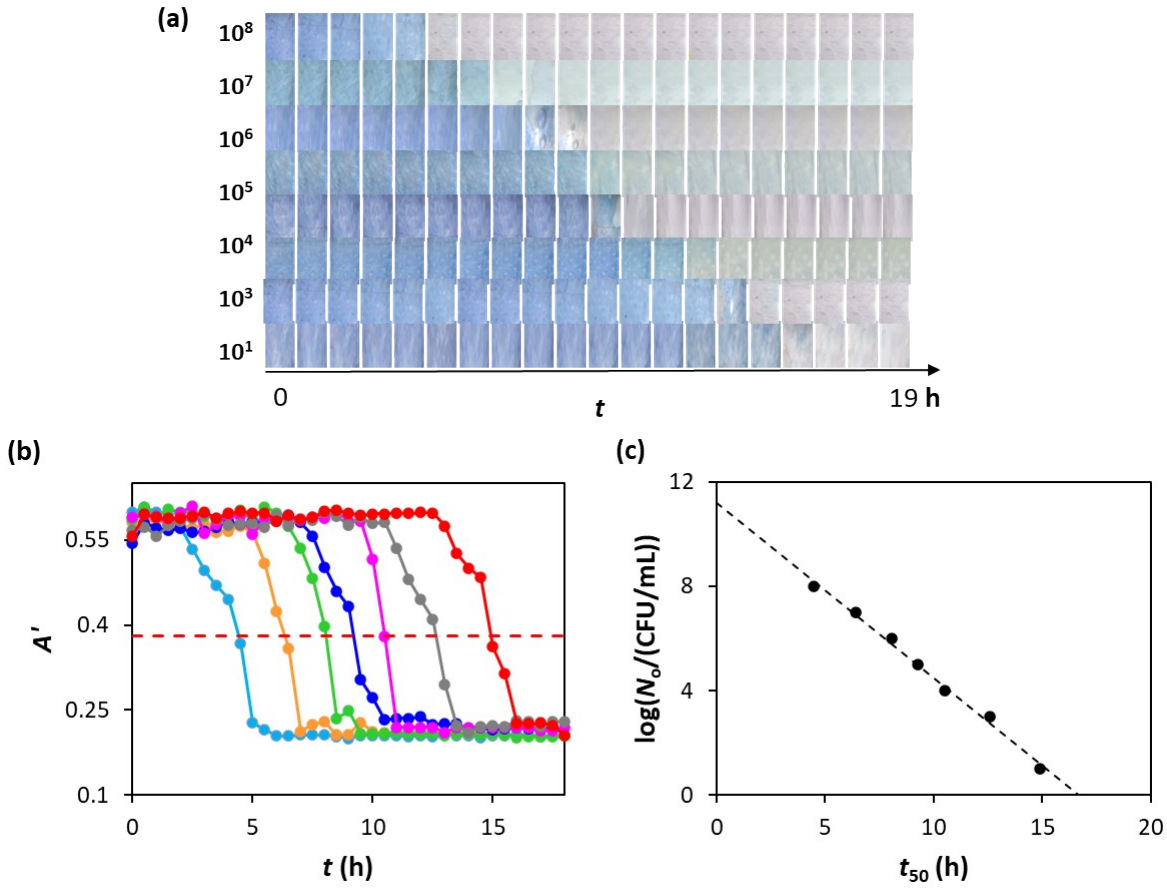

Fig. S19. (a) Photographic images of the H_2 indicator as a function of incubation time, *t*, in a typical set of H_2 μR-TVC runs, in which the 9 mL of growth medium were inoculated with a 1 mL *E. cloacae* sample with a bacterial load spanning the range (from left to right), 10^8 – 10^1 CFU/mL. (b) *A'* vs *t* reverse 'S' shaped profiles calculated from the photos illustrated in (a) using DCA and eqn (4), for initial inocula of (from left to right): 10^8, 10^7, 10^6, 10^5, 10^4, 10^3, 10^2 and 10^1 CFU/mL, respectively. (c) Subsequent straight line, calibration graph plot of $\log(N_o/(\text{CFU/mL}))$ vs t_{50}, derived from (b). Incubation temperature: 37 °C.

C. bifermentans

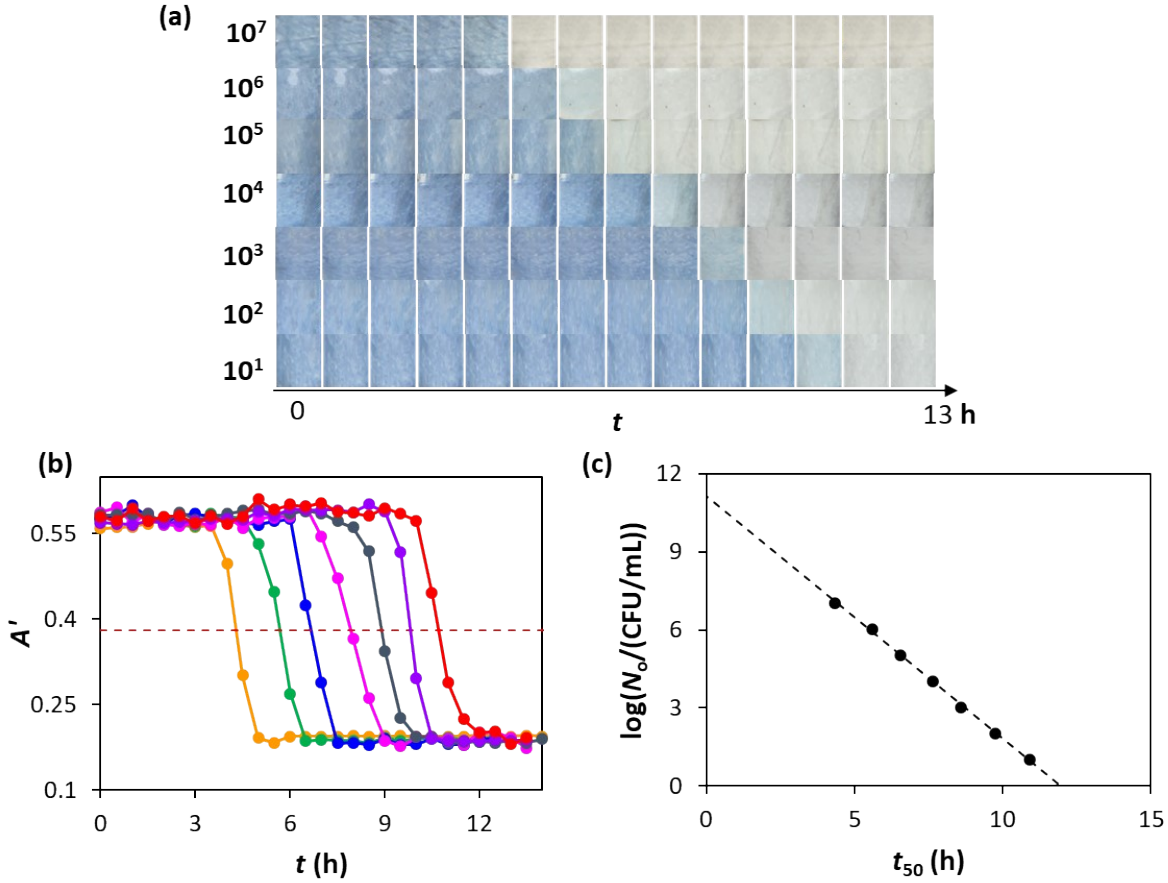

Fig. S20 (a) Photographic images of the H_2 indicator as a function of incubation time, *t*, in a typical set of H_2 μR-TVC runs, in which the 9 mL of growth medium were inoculated with a 1 mL *C. bifermentans* sample with a bacterial load spanning the range (from left to right), 10^7 – 10^1 CFU/mL. (b) *A'* vs *t* reverse 'S' shaped profiles calculated from the photos illustrated in (a) using DCA and eqn (4), for initial inocula of (from left to right): 10^7, 10^6, 10^5, 10^4, 10^3, 10^2 and 10^1 CFU/mL, respectively. (c) Subsequent straight line, calibration graph plot of $\log(N_o/(\text{CFU/mL}))$ vs t_{50}, derived from (b). Incubation temperature: 37 °C.

S11 Comparison of H_2 and O_2 microrespirometry of *E. coli*

As noted in the main script, under initial aerobic conditions, the evolution of H_2 appears to occur after all the dissolved O_2 has been consumed by the bacteria, when an inoculum of 10^4 CFU/mL *E. coli* was used. This would suggest that it is likely the O_2 microrespirometry τ vs t curves for a range of different inoculum concentrations of *E. coli*, would be occur at roughly the same time earlier (ca. 2 h) than the A' vs t curves, illustrated in Fig. 4(b). To demonstrate this, the τ vs t curves generated using an O_2 sensor under otherwise the same reaction conditions as those used in Fig. 4 were recorded and are illustrated in Fig. S21(a)

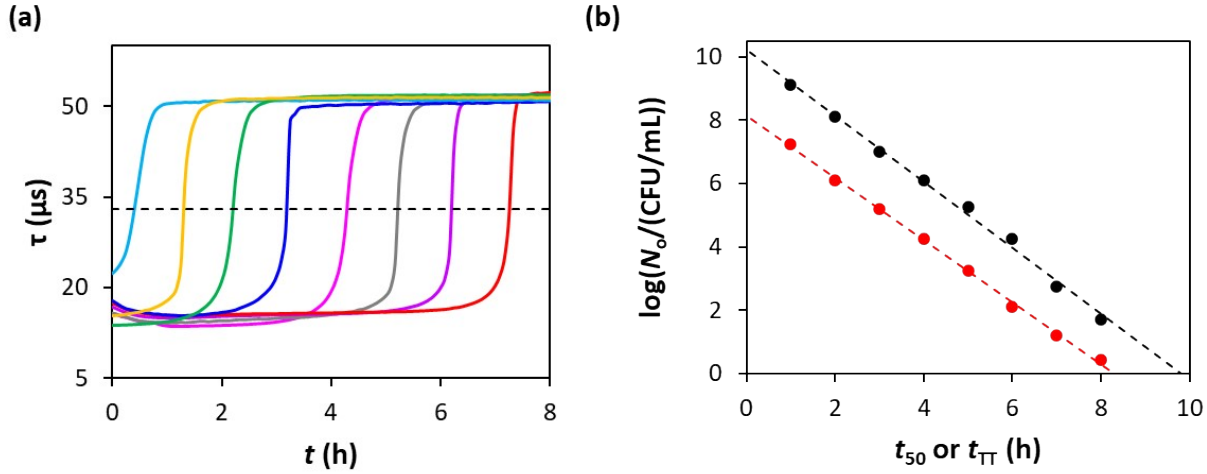

Fig. S21 (a) O_2 indicator lifetime, τ, vs t profiles in a typical set of O_2 μR-TVC run, in which the 9 mL of anaerobic growth medium were inoculated with a 1 mL *E. coli* sample with a bacterial load spanning the range (from left to right), 10^8, 10^7, 10^6, 10^5, 10^4, 10^3, 10^2 and 10^1 CFU/mL, respectively. (b) Subsequent straight line, calibration graph plot of $\log(N_o/(\text{CFU/mL}))$ vs t_τ derived using data in (a), red points, and $\log(N_o/(\text{CFU/mL}))$ vs t_{50}, from Fig. 4(c), black points. Incubation temperature: 37 °C.

From each of these profiles a value of t_{TT} (the incubation time when τ was halfway through its change) was determined and used to generate the subsequent straight-line plot of $\log(N_o)$ vs t_{TT} illustrated in Fig. S21(b) (red points). Also shown in this diagram is the straight-line plot of $\log(N_o)$ vs t_{50} results (black points) generated by the H_2 indicator under the same experimental conditions. These two straight line plots are approximately parallel, with a time gap of ca. 2 h, which supports the proposition that in this H_2 evolving system at least H_2 evolution follows shortly after all the dissolved O_2 has been consumed and the solution n rendered anaerobic.